



Article

Direct Hydroxylation of Phenol to Dihydroxybenzenes by H₂O₂ and Fe-based Metal-Organic Framework Catalyst at Room Temperature

Alma D. Salazar-Aguilar ^{1,2}, Gonzalo Vega ², Jose A. Casas ², Sofía Magdalena Vega-Díaz ¹, Ferdinando Tristan ¹ , David Meneses-Rodríguez ³ , Manuel Belmonte ⁴ and Asunción Quintanilla ^{2,*}

¹ Departamento de Ingeniería Química, Tecnológico Nacional de México, Instituto Tecnológico de Celaya, Av. García Cubas Pte # 600 esq. Avenida Tecnológico, Celaya 38010, Guanajuato, México; daniela.salazar@iqcelaya.itc.mx (A.D.S.-A.); sofia.vega@iqcelaya.itc.mx (S.M.V.-D.); ferdinando.tristan@iqcelaya.itc.mx (F.T.)

² Chemical Engineering Department, Universidad Autónoma de Madrid, Ctra. Colmenar km 15, 28049 Madrid, Spain; gonzalo.vega@uam.es (G.V.); jose.casas@uam.es (J.A.C.)

³ Cátedras-CONACYT CINVESTAV – Mérida, Ctra. Antigua a Progreso Km 6, Cordemex 97310, Mérida, Yucatán, México; david.meneses@gmail.com

⁴ Institute of Ceramics and Glass (ICV-CSIC), Campus de Cantoblanco, Kelsen 5, 28049 Madrid, Spain; mbelmonte@icv.csic.es

* Correspondence: asun.quintanilla@uam.es; Tel.: +34-914-973-454

Received: 31 December 2019; Accepted: 28 January 2020; Published: 2 February 2020



Abstract: A semi-crystalline iron-based metal-organic framework (MOF), in particular Fe-BTC, that contained 20 wt.% Fe, was sustainably synthesized at room temperature and extensively characterized. Fe-BTC nanopowders could be used as an efficient heterogeneous catalyst for the synthesis of dihydroxybenzenes (DHBZ), from phenol with hydrogen peroxide (H₂O₂), as oxidant under organic solvent-free conditions. The influence of the reaction temperature, H₂O₂ concentration and catalyst dose were studied in the hydroxylation performance of phenol and MOF stability. Fe-BTC was active and stable (with negligible Fe leaching) at room conditions. By using intermittent dosing of H₂O₂, the catalytic performance resulted in a high DHBZ selectivity (65%) and yield (35%), higher than those obtained for other Fe-based MOFs that typically require reaction temperatures above 70 °C. The long-term experiments in a fixed-bed flow reactor demonstrated good Fe-BTC durability at the above conditions.

Keywords: Fe-BTC; MOF; phenol hydroxylation; dihydroxybenzenes; selective oxidation

1. Introduction

The hydroxylation of phenol to catechol (CTL) and hydroquinone (HQ) is a prominent industrial reaction. The obtained dihydroxybenzenes (DHBZ) have several applications, such as polymerization inhibitor, antioxidant, precursor to drugs, perfumes, etc. [1–3]. The most acceptable reaction employs hydrogen peroxide (H₂O₂) as the oxidant and a heterogeneous catalyst. Titanium silicalite zeolites (TS-1), is the catalyst used in the commercial process developed by Enichem, in which a selectivity and yield of DHBZ of around 94 and 25%, respectively, are achieved at 70–100 °C [4,5]. The catalyst regeneration is considered in the process due to its deactivation by deposition of polymers or tar on the TS-1 surface [6]. For this reason, there is still much effort being taken to design new catalysts to improve the phenol hydroxylation performance.

Iron (Fe) is the preferred catalyst in the synthesis of DHBZ due to its low toxicity and cost, and because it exhibits a high activity in the decomposition of H_2O_2 into hydroxyl radical species, $\text{HO}\bullet$, responsible for phenol hydroxylation [7–9]. Decorated Fe materials have been explored in previous reports, but they deal with a poor active site dispersion that reduces their activity [10]. Metal–organic frameworks (MOFs) are novel hybrid materials constructed from organic ligands and inorganic metal ions. Due to their inherent porosity and well dispersed active sites, MOFs are potential catalysts in a wide number of reactions [11–14]. Generally, MOFs are synthesized by solvothermal methods in corrosive mediums— HNO_3 or HF solutions—during long time periods and at high temperatures [15–17]. Lately, new environmentally favorable synthesis methods have been reported [11,18], allowing the use of MOFs in some large-scale applications. Nonetheless, this method usually sacrifices some properties like crystallinity or porosity [19]. Despite this, these simplified methods are ideal, as a minimum of hazardous residues are produced. Large-scale production of MOFs is required due to the wide number of fields in which they are employed, for instance, in photocatalysis [20], electrochemistry [21], as adsorbents [22], and in gas separation [23]. However, the key issue in view of their actual application is the stability of the MOF-based catalysts, in particular when liquid phase media are involved [24]. This necessitates the examination of the stability of MOF catalysts under a wider range of operational conditions in order to select those that avoid the leaching of the metals.

Recently, MOFs with different metal active sites have been reported as catalysts for the hydroxylation of phenol [25–28]. For instance, Cu-MOF $[\text{Cu}_2(\text{BPTC})(\text{Im})_4]$ (H_4BPTC = Bypenyl-3, 3', 4, 4'-tetracarboxylic acid, Im = imidazole) was synthesized by a hydrothermal method and tested for phenol hydroxylation at 30–50 °C using a phenol: H_2O_2 molar concentration ratio equal to 1.0:1.8, ethanol:water 4:1 and 0.04 g of the catalyst. The catalyst was not active at temperatures below 40 °C, but at this temperature, the DHBZ selectivity and yield were 94 and 24% after 4 h of reaction. The amount of Cu leached was not monitored [25].

MOF-5 (Ni) [Zn-Ni coordinated to phenylenedimethylene] exhibited activity only after doping with Fe(III) ions. At 80 °C, and using an excess of H_2O_2 , the reaction yields to CTL were 29–63%, depending on the Fe mass content in the catalyst, showing a selectivity to DHBZ of 100%. Neither HQ nor other aromatic components were detected in the reaction media, but the presence of tar was not evaluated in the study. The Fe leached was from 1.8 to 6.0% of initial Fe after 1 h, depending on the operating conditions, and the catalyst synthesis required solvents that increased risks and production cost [26]. A similar material was also synthesized using Fe(II) to decorate MOF-5 [27]; in this case, the catalyst was less stable and 18% of the Fe was leached out after 2 h, using the same conditions as Fe(III)/MOF-5.

Bhattacharjee et al. [28] reported the application of Fe-MOF-74 $[\text{Fe}(\text{II})(\text{bhBDC})]$ (H_2bhBDC = 2,5-dihydroxy-1,4-benzenedicarboxylic acid), loaded with 30 wt.% Fe, for the hydroxylation of phenol at 20 °C and using a phenol: H_2O_2 concentration ratio of 1:1. The DHBZ selectivity and yield were 44 and 26%, respectively. The Fe leached was not considered, but after 10 min of reaction, there were not significant changes in the concentration of reactants and products. It is likely that the hydroxylation stopped due to the total consumption of H_2O_2 . The particularly fast decomposition of H_2O_2 at 20 °C suggests that Fe was in the liquid media.

In this work, a MOF of Fe(III) and trimesic acid (H_3BTC), Fe-BTC, has been synthesized at room temperature by using a stirring method in water solution and, afterwards, it was evaluated in the hydroxylation of phenol. The synthesized Fe-BTC MOF was physically and chemically characterized by nitrogen physisorption, X-ray diffraction (XRD), differential scanning calorimetry (DSC), total reflection X-ray fluorescence (TXRF), scanning electron microscopy (SEM), X-ray photoelectron spectroscopy (XPS), Fourier-transform infrared spectroscopy (FTIR) and thermogravimetric analysis (TGA). The hydroxylation of phenol reaction was studied under different operating conditions (i.e., temperature, phenol: H_2O_2 concentrations ratio and catalyst dose). The carbon mass balance was matched thanks to the use of appropriate analytical techniques such as high-performance liquid

chromatography (HPLC) and total organic carbon (TOC) of the liquid phase and TGA of the used catalyst. The Fe-BTC stability was suitably tested by using a continuous fixed-bed reactor. According to the results, herein it is proved that Fe-BTC is an active and durable catalyst for the hydroxylation of phenol at room temperature (20–25 °C). Interestingly, Fe leaching is totally avoided by using an intermittent dosing of H_2O_2 .

2. Results and discussion

2.1. Catalyst Characterization

The XRD pattern of Fe-BTC powder is presented in Figure 1a. The diffractogram shows wide and weak amorphous halos instead of well-defined and narrow peaks. This indicates the expected semi-crystalline nature of the material due to the mild synthesis conditions that prevent crystallization in some areas; also, the pattern is similar to the one reported previously by Sanchez-Sanchez et al. [29]. It is expected that the observed defects in crystallinity could improve the accessibility of the Fe sites due to their unsaturated nature [19].

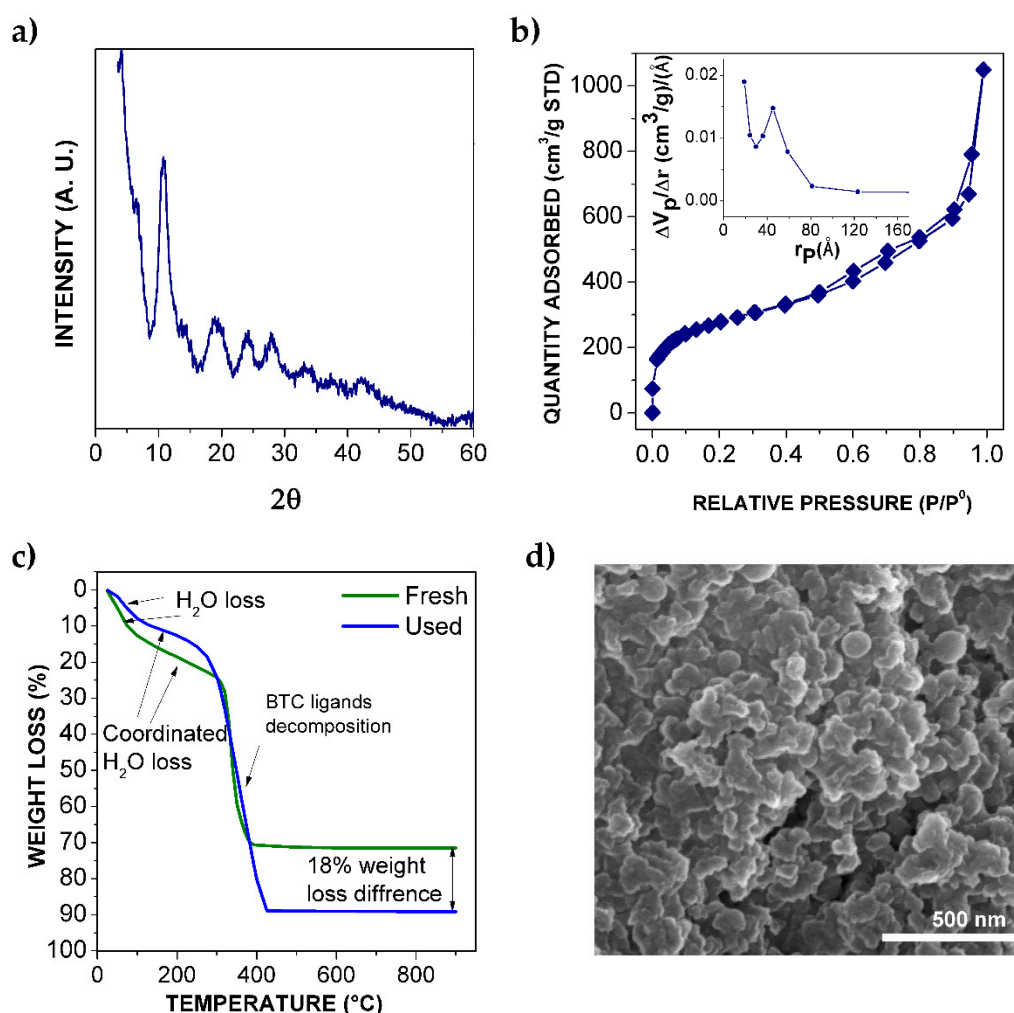


Figure 1. Fe-BTC physical characterization: (a) X-ray diffraction (XRD) pattern; (b) adsorption isotherm of N_2 , inset: micropore size distribution by BJH method; (c) thermogravimetric analysis (TGA) curves before (fresh) and after reaction (used); (d) SEM micrograph of Fe-BTC powder.

Surface area was estimated by N_2 physisorption. The isothermal curve, characteristic of micropore and mesopore materials [30], is observed in Figure 1b. Fe-BTC presented a BET surface value of

$975 \text{ m}^2\cdot\text{g}^{-1}$, where the external surface of the powders had $929 \text{ m}^2\cdot\text{g}^{-1}$. The inset of Figure 1b shows the micropore size distribution, calculated by BHJ Desorption Pore Distribution, where an average pore width of 73 \AA was estimated.

Thermal stability of Fe-BTC was studied by TGA under air atmosphere before and after the reaction of hydroxylation of phenol. Figure 1c shows the TGA profiles of both materials. As well as this, the DSC curves are provided in Figure S1 (see Supplementary Information). The first weight loss of the fresh catalyst, at near 100°C , was attributed to the release of water, and likely ethanol, that could remain from the synthesis (which could also explain why the BET surface area was slightly lower than reported by Sanchez-Sanchez et al. [29]). A new weight loss step was observed around 200°C , which can be assigned to adsorbed water in the cages of Fe-BTC [18]. At around 300°C , the organic ligand BTC burnt out [11], leading to a 48% weight loss of the original sample. The remaining mass after the analysis was 28% and, assuming that it mostly corresponds to Fe_2O_3 , it is possible to estimate an initial Fe content of 20 wt.% in the fresh Fe-BTC. This value was also confirmed by TXRF.

A SEM micrograph of Fe-BTC particles (Figure 1c) evidenced their nano-size ($\sim 50\text{--}100 \text{ nm}$) and spherical morphology. Agglomerates can also be seen, indicating that nanoparticles are attracted to each other due to surface interactions.

The FTIR spectrum, in Figure 2a, confirmed the coordination among Fe metal sites and organic ligands in the Fe-BTC. The bands corresponding to C=C vibration, located at 1362 and 1451 cm^{-1} , are observed in both the precursor H_3BTC and the synthesized Fe-BTC nanopowders. Moreover, the band at 1109 cm^{-1} is related to the metalorganic group C-O-Fe [31]. This information verifies the MOF nature of Fe-BTC material, in agreement with the XRD pattern previously reported.

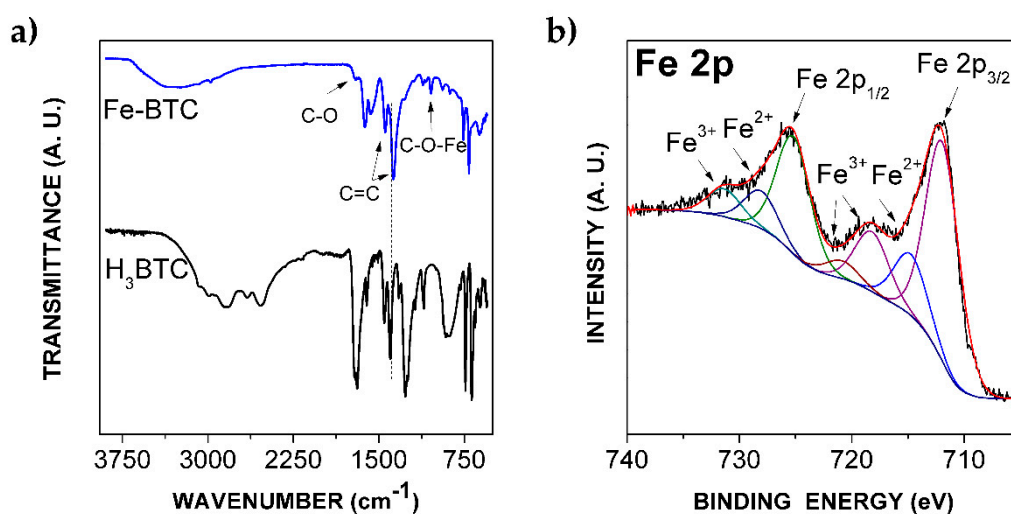


Figure 2. (a) FTIR spectra of the precursor H_3BTC and synthesized Fe-BTC; (b) XPS spectrum and deconvolution of Fe 2p peaks of the Fe-BTC.

Additionally, the Fe oxidation state at the outermost surface of the MOF was determined by analyzing the XPS signal in the Fe 2p region. The spectrum is provided in Figure 2b. Two main peaks located at 711.9 and 725.2 eV were clearly observed and ascribed to Fe $2p_{3/2}$ and $2p_{1/2}$ cationic species, respectively [32]. The two satellite bands attributed to Fe^{2+} are located at 714.7 and 728 eV; the satellite bands corresponding to Fe^{3+} are located at 718.2, and 731.3 eV [32]. Both ionic states of Fe are catalytically active in the decomposition of H_2O_2 [7]. The overall Fe content on the outermost surface of the MOF, calculated from the deconvolution of the main XPS peaks is 1 at. %, which implies that most of the Fe content is located inside MOF cages.

2.2. Hydroxylation of Phenol

The prepared Fe-BTC was tested as a catalyst in the hydroxylation of phenol using H_2O_2 as an oxidant by varying the most affecting operational parameters viz. temperature, H_2O_2 concentration and catalyst dose [25–28,33]. Water was the only solvent used. Figure 3 shows the typical conversion-time profile of phenol and concentration-time profiles of H_2O_2 (Figure 3a) and the various components involved in the reaction (Figure 3b,c), such as CTL, HQ, p-benzoquinone (BQ) and resorcinol (RSL). From these results, and according to Equations (1–3), the molar selectivity to HQ, CTL and DHBZ, as well as the yield to DHBZ at different phenol conversions, were calculated and represented in Figure 4a.

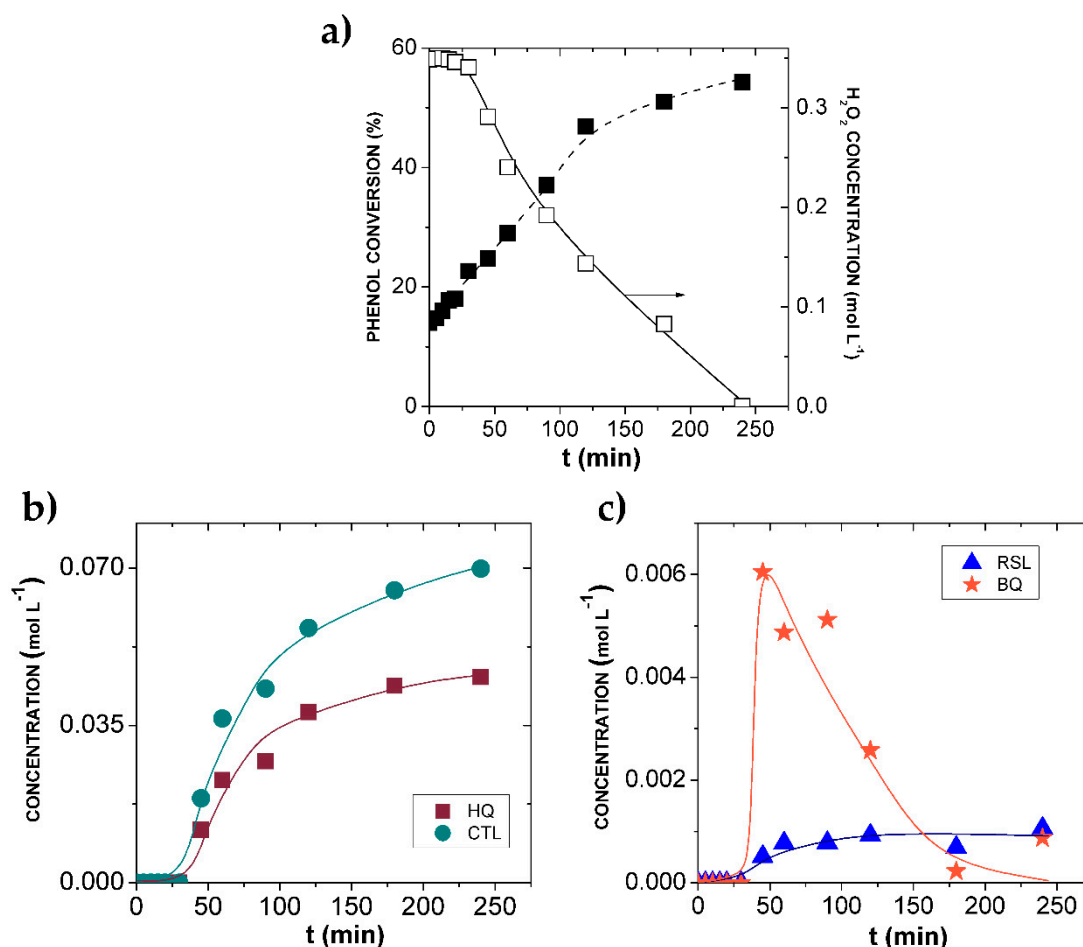


Figure 3. Results of the hydroxylation of phenol over Fe-BTC in a batch reactor. (a) Temporal profiles of phenol conversion and H_2O_2 concentration; (b) temporal profiles of CTL and HQ (c) and BQ and RSL concentration. Operating conditions: $[\text{Phenol}]_0 = 0.35 \text{ mol L}^{-1}$, $[\text{H}_2\text{O}_2]_0 = 0.35 \text{ mol L}^{-1}$, $T = 20^\circ\text{C}$, $W_{\text{FeBTC}} = 0.010 \text{ g}$.

As can be seen, there is an induction period that, at the particular operating conditions of Figure 3 ($T = 20^\circ\text{C}$, $W = 0.01 \text{ g}$ and 1:1 molar), is equivalent to 25 min. During this time, the phenol uptake is due to its adsorption on the Fe-BTC surface (around 20% of the initial concentration), while H_2O_2 is not decomposed and oxidation products are not detected. The same phenol uptake was obtained in a control experiment carried out at the same operating conditions but in the absence of the oxidant. After this lapse, in which the catalyst has been saturated in phenol, the decomposition of H_2O_2 into $\text{HO}\bullet$ species began and the concentration of both CTL and HQ started to increase. RSL and BQ were also detected, but their concentration was one order of magnitude lower than CTL and HQ. Notably, the maximum in the BQ concentration profile was achieved at around 50 min of reaction. According to

this, DHBZ are the final products, whereas BQ is an intermediate component, and it can further react to more complex molecules, such as unwanted tar products [25,34].

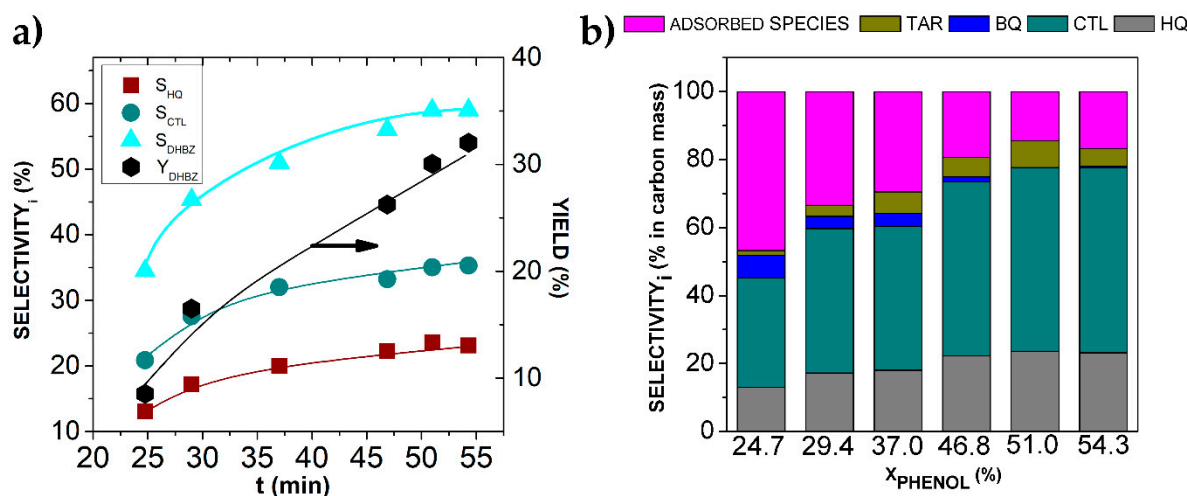


Figure 4. (a) Evolution of the molar selectivity and yield to DHBZ upon the hydroxylation of phenol over Fe-BTC in a batch reactor; (b) carbon mass distribution upon the hydroxylation of phenol over Fe-BTC. Operating conditions: $[Phenol]_0 = 0.35 \text{ mol L}^{-1}$, $T = 20 \text{ }^{\circ}\text{C}$, $W_{FeBTC} = 0.01 \text{ g}$.

After 4 h of reaction at $20 \text{ }^{\circ}\text{C}$, once H_2O_2 was completely consumed, the phenol conversion was 54% (Figure 3a) and the selectivity to DHBZ (S_{DHBZ}) 55% (Figure 4a). The molar ratio CTL:HQ remained at 1.5 (Figure 4a). These results lead to DHBZ yield (Y_{DHBZ}) of 33%. This performance can be exclusively attributed to the Fe-BTC catalytic activity, since it was verified that the liquid-phase reaction (in absence of catalyst) did not take place at $20 \text{ }^{\circ}\text{C}$, and the contribution of the leached Fe (as high as 1.6 ppm after 3 h of reaction) was negligible (Figure 3a). As far as we know, this is the highest selectivity and yield value reported in the hydroxylation of phenol at $20 \text{ }^{\circ}\text{C}$ using water as a solvent. The work by Bhattachajee et al. [28] reported activity of the Fe-MOF-74 catalyst at this temperature (S_{DHBZ} and Y_{DHBZ} of 44 and 26%, respectively), but with some uncertainty about the extension of the reaction in the liquid phase by leached Fe.

After the reaction, the amount of physisorbed and occluded water in the used Fe-BTC was a 10% higher than in the fresh one, as is observed in the TGA curve of the used catalyst (Figure 1c). In addition, weight loss at $300 \text{ }^{\circ}\text{C}$ was significantly higher, corresponding to 66% of the initial material, and an additional 18% with respect to the fresh catalyst, a value that is coincident with the amount of carbon-adsorbed species estimated by TOC after the reaction (Figure 4b). This confirms the presence of organic matter adsorbed on the Fe-BTC surface upon reaction. In fact, DSC curves for the fresh and used Fe-BTC catalyst show a wider exothermic heat flow peak in the latter (Figure S1). The wide peak, involving temperatures from 290 to $410 \text{ }^{\circ}\text{C}$, could indicate the presence of more complex molecules or high molecular weight species (such as tar products) adsorbed on the Fe-BTC surface. Consequently, the BET surface area decreased from 975 to $304 \text{ m}^2\text{g}^{-1}$. The narrower pores were blocked and now the average pore width, estimated by the same BJH method, was 135 \AA (see Figure S2 of the Supporting Information).

To gain an insight into the products' distribution, the TOC of the reactor liquid samples was also analyzed and the results were compared to the calculated TOC values from the identified components (phenol, CTL, HQ, BQ and RSL). The differences were attributed to the sum of the unidentified carbon present in the liquid phase and other more complex species, such as tar. The difference between the initial TOC (corresponding to phenol concentration of 0.35 mol L^{-1}) and the measured TOC in the liquid sample provides the amount of carbon adsorbed on the Fe-BTC surface. Overall, the selectivity distribution in terms of carbon mass is shown in Figure 4b. The progressive production

of tar is clearly observed, while BQ disappears. The tar selectivity ranged from 1 to 7% in carbon mass. The initial amount of adsorbed species is as much as 50% and is reduced by up to 17% upon reaction. Initially, the adsorbed species were mainly phenol, that is progressively hydroxylated to CTL, and HQ (Figure 4b). At the end of the reaction (phenol conversion of 54% and total consumption of H_2O_2), the adsorbed phenol seems to evolve into more complex molecules, also postulated as the tar component, according to the broad peak detected by DSC-TGA (Figure S1). Upon reaction, CTL and HQ became the major components, and 70% of the phenol initial carbon was finally converted into them.

2.2.1. Influence of Operating Conditions

The catalytic performance of Fe-BTC nanopowders was evaluated at different reaction temperatures (20–50 °C), H_2O_2 concentrations (phenol: H_2O_2 molar ratios from 1:1.8 to 1:0.5) and masses of catalyst (0.02–1 g L^{-1} , entries 3, 9 and 10). Table 1 summarizes the results of the phenol hydroxylation and H_2O_2 consumption for different times over 180 min of reaction. Likewise, the initial induction time and the Fe leaching at the given reaction time were also included. As can be seen, the three operating conditions studied affected both the hydroxylation performance and the catalyst stability.

Table 1. Catalytic performance of Fe-BTC upon the hydroxylation of phenol at different operating conditions.

Entry	T (°C)	PHENOL : H_2O_2	W_{CAT} (g)	$t_{\text{INDUCTION}}$ (min)	CONVERSION (%)			SELECT. (%)		YIELD (%) HQ+CTL	Fe_{lix} (ppm)
					t_{R} (min)	PHENOL	H_2O_2	HQ	CTL		
1	50	1:1	0.01	0	10	52.3	100	33.0	41.7	39.7	26
2	25	1:1	0.01	25	60	51.0	68.5	20.3	37.4	29.4	17
3	20	1:1	0.01	25	60	29.4	31.4	17.4	27.5	13.2	0.4
4	20	1:1.8	0.01	25	60	37.0	14.8	18.0	29.5	17.6	1.2
5	20	1:0.5	0.01	25	60	26.0	34.2	25.0	32.7	15.0	0
6	20	1:1.8	0.01	25	180	61.7	55.0	24.7	36.7	37.9	10
7	20	1:1	0.01	25	180	50.7	78.6	23.6	35.0	29.7	1.6
8	20	1:0.5	0.01	25	180	37.8	93.9	25.2	39.0	24.3	2.0
9	20	1:1	0.02	20	60	34.1	46.2	30.2	44.2	25.4	2.0
10	20	1:1	0.05	15	60	52.2	95.2	35.0	44.3	41.4	24

The first set of experiments was performed at 20, 25 and 50 °C ($\text{W}_{\text{FeBTC}} = 0.01$ g and phenol: H_2O_2 1:1, entries 1–3 of Table 1). The increase in temperature promoted a faster H_2O_2 decomposition into radical species, which was accompanied by faster phenol hydroxylation (Table 1). At a given phenol conversion (around 51%, see Entry 1 and 2), the S_{DHBZ} was affected by the temperature, being 74.7 and 62.8% for 50 °C (Entry 1) and 25 °C (Entry 2), respectively. On the other hand, a significant amount of Fe dissolved in the reaction media was detected from 25 °C, being the main cause of the observed reaction (as deduced from a control experiment, carried out by loading the batch reactor with 17 ppm of Fe as FeCl_2 at 25 °C). These results indicate that the reaction temperature is critical for the catalyst stability. Then, a temperature of 20 °C was fixed to continue the study in order to exclude, as much as possible, the homogeneous contribution by the Fe leached.

The H_2O_2 concentration was used at 0.63, 0.35 and 0.17 mol L^{-1} , corresponding to a phenol: H_2O_2 ratios of 1:1.8, 1:1 and 1:0.5, respectively ($\text{W}_{\text{FeBTC}} = 0.01$ g and $T = 20$ °C, entries 3–8). The H_2O_2 dose influenced the phenol conversion but also the efficient consumption of this oxidant ($\text{H}_2\text{O}_{2\text{eff}}$ defined as mol of phenol converted to products per initial mol of H_2O_2). Thus, at the highest H_2O_2 dose, see entry 4 of Table 1 at a phenol: H_2O_2 ratio equal to 1:1.8, the phenol conversion was 37% and the $\text{H}_2\text{O}_{2\text{eff}}$ 23%; while at a lower H_2O_2 dose (Entry 5 of Table 1), with a phenol: H_2O_2 ratio equal to 1:0.5, the phenol diminished to 26% and the H_2O_2 efficiency was significantly increased, up to 52%. Furthermore, at similar phenol conversions, 29.4 and 26% for 1:1 (Entry 3) and 1:0.5 (Entry 5), respectively (also at 60 min), the S_{DHBZ} is enhanced from 45 to 57.7%. That is, at low H_2O_2 concentrations, efficiency in the consumption of H_2O_2 and the S_{DHBZ} was improved. These findings suggest that a lower concentration of $\text{HO}\bullet$ species, and consequently of the phenoxy radicals ($\text{RO}\bullet$) generated upon reaction [35], favors

the hydroxylation versus unwanted condensation reaction towards tar production. Besides, a low H_2O_2 concentration is also beneficial for the Fe-BTC stability. In fact, 10 ppm of Fe was dissolved at a high dose of H_2O_2 and under long reaction times (compare Entry 6 with Entries 7 and 8). In conclusion, the use of high phenol: H_2O_2 ratios (or low H_2O_2 dose) is recommended in the hydroxylation of phenol in order to reduce the tar production and the Fe leaching.

The mass of catalyst was varied at 0.01 (Entry 3), 0.02 (Entry 9) and 0.05 (Entry 10) g (phenol: H_2O_2 equal to 1:1 and $T = 20\text{ }^\circ\text{C}$). The higher the amount of catalyst load to the reactor, the higher the amount of Fe dissolved. This Fe in solution accelerated H_2O_2 decomposition and, consequently, phenol conversion. However, S_{DHBZ} was not apparently affected, which supports the idea that an accumulation of the $\text{HO}\bullet$ species promoted unwanted reactions. At 0.01 and 0.02 g (Entries 3 and 9, respectively), when leaching was negligible, the $\text{H}_2\text{O}_{2\text{eff}}$ was 34 and 43%, respectively, which indicates that the tar production does not necessarily takes place in the liquid phase by the Fe dissolved. The mentioned $\text{HO}\bullet$ accumulation is not only due to the Fe in the liquid phase.

In conclusion, the amount of Fe leached limits the feasibility of the Fe-BTC catalyst in the hydroxylation of phenol by H_2O_2 . The operating conditions govern the catalyst stability and, as has been demonstrated, low temperatures, H_2O_2 doses and a catalyst load are required ($T < 25\text{ }^\circ\text{C}$, phenol: $\text{H}_2\text{O}_2 \leq 1:1$ and $W \leq 0.02\text{ g}$). On the other hand, the concentration of $\text{HO}\bullet$ species in the reaction media (liquid phase and catalyst surface) seems to play a main role in the phenol selectivity to DHBZ, in such a way that a fast H_2O_2 decomposition leads to a lower S_{DHBZ} by favoring undesirable condensation reactions. In this sense, the pulse dosage of the H_2O_2 could be an attractive control option. It would also be expected that this strategy favors Fe-BTC stability. For these reasons, the hydroxylation of phenol at $25\text{ }^\circ\text{C}$, phenol: $\text{H}_2\text{O}_2 = 1:1$ and 0.01 g of catalyst was carried out during 180 min by feeding the required H_2O_2 concentration in three equal doses, at 0, 60 and 180 min of reaction. The reaction at $25\text{ }^\circ\text{C}$ was selected because, from an industrial process point of view, it is more cost effective to work at room conditions than below or above room temperature. The evolution of S_{DHBZ} and Y_{DHBZ} with the phenol conversion is given in Figure 5. As can be seen, S_{HQ} and S_{CTL} were 25 and 40%, respectively, when phenol conversions from 40 to 60% were achieved. This means that S_{DHBZ} and Y_{DHBZ} values of 65% of 35%, respectively, were achieved. Notably, the Fe leached was null upon 180 min of reaction, in contrast to the 17 ppm of Fe detected at this temperature when H_2O_2 was introduced from the beginning of the reaction (Table 1).

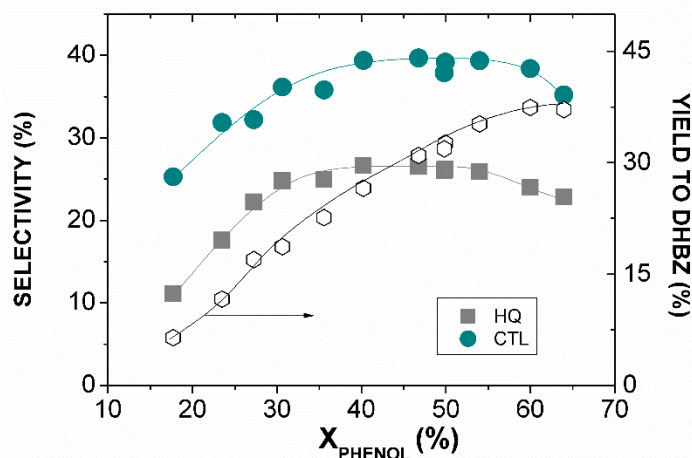


Figure 5. Results of the hydroxylation of phenol over Fe-BTC with H_2O_2 dosage. Operating conditions: $[\text{Phenol}]_0 = 0.35\text{ mol L}^{-1}$, phenol: $\text{H}_2\text{O}_2 = 1:1$, $T = 25\text{ }^\circ\text{C}$, $W_{\text{FeBTC}} = 0.01\text{ g}$.

As far as we know, this is the best performance reported for the hydroxylation of phenol in water at room conditions. The Fe-BTC activity is clearly superior to that exhibited by other MOF catalysts, based on Fe and Cu, that require higher temperatures for the reaction [25–27]. Therefore, the Fe-BTC

MOF is a valuable and suitable catalyst for the production of DHBZ, and its use must be accompanied by an adequate process strategy to guarantee the catalyst's stability.

2.2.2. Stability and performance in continuous fixed-bed reactor

The stability of the Fe-BTC was studied in an up-flow fixed bed reactor for 6 h on stream. For this, the hydroxylation of phenol was performed at room temperature (25 °C), with two initial concentrations of H_2O_2 and a significantly low space-time, $\tau = 1.7 \text{ g h L}^{-1}$ (equivalent to 0.5 min of residence time). The results are provided in Figure 6. As can be seen, once it overpassed the initial adsorption period of 0.5–1 h, the phenol conversion remained constant during the 6 h test. On the other hand, the stationary stage for the DHBZ was reached later (after 2 h of time on stream), due to the initial enhanced phenol uptake by the adsorption contribution. The results of the performance at phenol: H_2O_2 molar ratio = 1:1 are similar to those obtained in the batch reactor at 25 °C, viz. 55% of phenol conversion, and HQ and CTL selectivities of 25 and 35%, respectively. In accordance with the effect of the H_2O_2 dose, at a 1:0.5 ratio the phenol conversion was lower and the selectivity slightly higher (Figure 6). Interestingly, the loss of Fe in the flow reactor was quite low compared to the performance of batch conditions, from 1 to 5 wt.% of what was initially loaded after 6 h on stream, and was the highest for the 1:1 ratio, as expected.

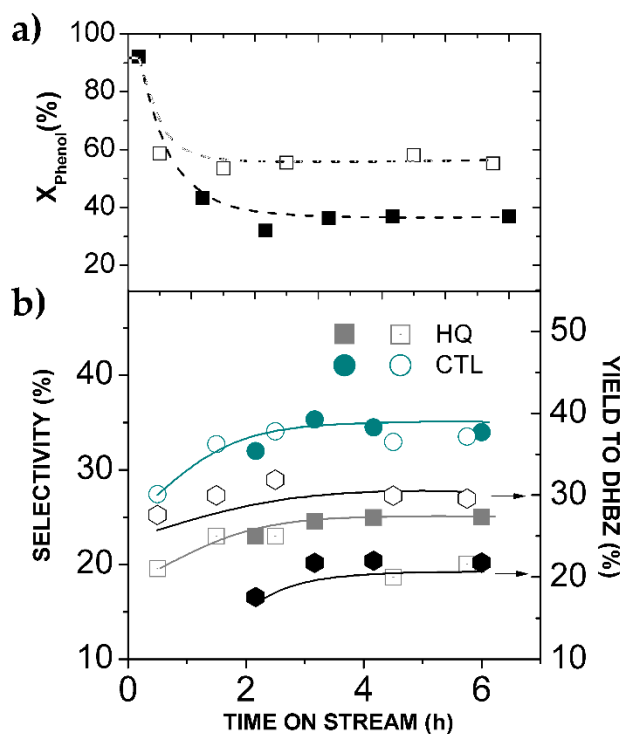


Figure 6. Results of the hydroxylation of phenol over Fe-BDT in a flow-reactor. (a) Evolution of phenol conversion and (b) evolution of phenol selectivity to hydroquinone (HQ) and catechol (CTL) and DHBZ yield with time on stream. Operating conditions: $[\text{Phenol}]_0 = 0.35 \text{ mol L}^{-1}$, $T = 25 \text{ }^\circ\text{C}$, $W_{\text{FeBTC}} = 0.025 \text{ g}$, $Q_L = 0.25 \text{ mL min}^{-1}$, $\tau = 1.7 \text{ g h L}^{-1}$. Open and close symbols: phenol: H_2O_2 = 1:1 and 1:0.5, respectively.

Taking into account that the performance was evaluated at 1.7 g h L^{-1} of space-time and 0.5 min of reaction time, the Fe-BTC turnover frequency (TOF) was equal to 2350 h^{-1} (0.6 s^{-1}) that clearly evidences the potential of Fe-BTC as a selective oxidation catalyst with H_2O_2 , and also opens the opportunity to use low-cost semi-crystalline MOFs for this type of reaction.

3. Materials and Methods

3.1. Materials

Iron(III) chloride (FeCl_3), trimesic acid (H_3BTC), phenol and hydrogen peroxide solution 30% (H_2O_2) were purchased from Sigma-Aldrich. Sodium hydroxide (NaOH) was obtained from Meyer and ethanol (EtOH) was purchased from Fermont. The working standard solutions of phenol, hydroquinone, resorcinol, catechol, p-benzoquinone, all from Sigma-Aldrich, were prepared and used for High Performance Liquid Chromatography (HPLC). All these reagents had an analytical grade and were used without further purification. All solutions were prepared with deionized water.

3.2. Synthesis of Catalyst

Fe-BTC MOF was prepared at room temperature by using a stirring method in water solution, previously reported [29]. Briefly, a 30 mL solution with 0.67 g of H_3BTC and 0.5 g of NaOH was magnetically stirred for a few minutes, and then a 30 mL solution with 0.76 g of FeCl_3 was added dropwise and allowed to react for 2 h. The precipitated solid was recovered by centrifugation and washed several times with water and EtOH . Then, the orange powder was dried at $60\text{ }^\circ\text{C}$ in air for 48 h. The obtained material was denoted as Fe-BTC.

3.3. Characterization of Catalyst

Fe-BTC material was characterized by several techniques. Crystallographic studies were obtained using a Bruker X-ray diffractometer, D- δ Advance, equipped with a monochromatic Cu-K α 1 source with a wavelength of 1.54 \AA . The 2θ analysis range was set from 5° to 60° . Surface area was determined by N_2 adsorption in a Micromeritics TriStar II 3020 physisorption equipment with degasification conditions at $120\text{ }^\circ\text{C}$ in vacuum for 3 h. Surface area determination was calculated by the Brunauer, Emmett and Teller (BET) method [30]. Fe-BTC was analyzed with a field emission scanning electron microscope (SEM, S-4700, Hitachi). X-ray emission spectroscopy (XPS) analysis of the material was performed in a K-ALPHA spectrometer (Thermo Scientific), using a monochrome Al-K α X-ray beam with 40 W. The deconvolution of the bands was carried out using CasaXPS software. Infrared spectra for the material were obtained using a Thermo Scientific NicoletTMiSTM5 Fourier transform infrared spectrometer, using the ATR mode. TGA thermograms were obtained in a TA Instruments Discovery STD 650, under air atmosphere with an air flow of $90\text{ mL}\cdot\text{min}^{-1}$ at a heating rate of $10\text{ }^\circ\text{C}\cdot\text{min}^{-1}$ from $30\text{ }^\circ\text{C}$ to $950\text{ }^\circ\text{C}$. The overall Fe content was determined by total reflection X-ray fluorescence (TXRF EXTRA II, Rich & Seifert), using a Si-Li detector in a TXRF Extra-II spectrometer.

3.4. Hydroxylation Performance

Batch-wise experiments were carried out in a magnetically stirred three-necked glass reactor equipped with a reflux condenser. In a typical experiment, 50 mL of 0.35 M phenol solution was placed in the reactor, along with the Fe-BTC powders. The content was heated to the desired temperature (IKA RCT basic). Once this temperature was reached, 1.8 mL of an adjusted concentration of H_2O_2 was injected, and then the stirring process at 770 rpm started. After 3 h of reaction, the heating was switched off and the flask cooled to room temperature in cold water. The testing conditions were: phenol: H_2O_2 ratio molar equal to 1:1.8, 1:1 and 1:0.5, $T = 20\text{--}50\text{ }^\circ\text{C}$ and catalyst concentration $= 0.2\text{--}1\text{ g}\cdot\text{L}^{-1}$. The maximum deviation for the duplicate experiments was usually less than 5%.

Long-term experiments were conducted in a fixed-bed reactor consisting of a quartz tube of 0.91 cm of internal diameter and 0.7 cm long (reactor volume, $V_R = 1.3\text{ cm}^3$), loaded with 0.025 g of Fe-BTC placed with glass wool and quartz beads. The reactor was fed with a solution of 0.35 M phenol and phenol: H_2O_2 ratio molar equal to 1:1 and 1:0.5 at room condition ($25\text{ }^\circ\text{C}$) and a flow rate (Q_L) $= 0.25\text{ mL}\cdot\text{min}^{-1}$, which implies a space-time (τ) $= 1.7\text{ g h L}^{-1}$, equivalent to 0.5 min of residence time.

Liquid samples were periodically withdrawn from the reactors and immediately injected in a vial (submerged in crushed ice) containing a known volume of cold distilled water. The diluted samples were filtered (0.45 µm Nylon filter), and subsequently analyzed by different techniques.

3.5. Analytical Methods

Phenol and aromatic intermediates' evolution along oxidation reactions was followed by HPLC (Ultimate 3000, Thermo Scientific) using a C18 5 µm column (Kinetex from Phenomenex, 4.6 mm diameter, 15 cm long) and a 4 mM H₂SO₄ aqueous solution as stationary and mobile phases, respectively. The quantification was performed at wavelengths of 210 and 246 nm. TOC was quantified with a TOC analyzer (Shimadzu TOC VSCH). H₂O₂ concentration was obtained by colorimetric titration TiOSO₄ method [36] using a UV2100 Shimadzu UV-vis spectrophotometer.

The activity of the catalyst was evaluated using the parameters given below:

- The conversion (X) of phenol and H₂O₂,

$$X_i = \frac{C_{0,i} - C_{t,i}}{C_{0,i}} \quad (1)$$

where C_{0,i} and C_{t,i} are the i initial molar concentration and the i concentration at a given reaction time, respectively; i refers to phenol or H₂O₂;

- The phenol selectivity (S),

$$S_i = \frac{C_i}{C_{0,phenol} \cdot X_{phenol}} \quad (2)$$

where C_i is the molar concentration of a particular product such as CTL, HQ, BQ, RSL or tar;

- The phenol yield (Y),

$$Y_i = \frac{S_i \cdot X_{phenol}}{100} \quad (3)$$

- The effective conversion of H₂O₂ is expressed by,

$$H_2O_{2eff} = \frac{(C_{CAT} + C_{HQ} + 2 \cdot C_{BQ} + C_{RSL})}{C_{0,H_2O_2}} \quad (4)$$

4. Conclusions

Fe-BTC MOF nanopowders, prepared by stirring method at room temperature, are an attractive catalyst candidate for the hydroxylation of phenol with H₂O₂. This catalyst allows the green and sustainable synthesis of DHBZ by conducting the reaction at room temperature in aqueous media. The selection of adequate operating conditions is crucial for the reaction performance and MOF stability. The operating conditions must guarantee a progressive production of HO• species from the H₂O₂ decomposition, avoiding the accumulation of these species, to favor hydroxylation over condensation reaction to unwanted tar products. On the other hand, the reaction temperature is the key factor for the Fe leaching. A process strategy to combine both requirements was developed to perform the reaction with intermittent H₂O₂ dosing at room conditions. Under these conditions, a DHBZ selectivity and yield of 65% and 35% respectively, are achieved (W_{FeBTC}=0.01 g, phenol:H₂O₂ 1:1) in the absence of Fe leached, which is an improved catalytic performance compared to previous results reported by other MOF materials tested in this kind of reaction. This work also opens the possibility to develop fixed-bed processes with Fe-BTC MOF for phenol hydroxylation.

Supplementary Materials: The following are available online at <http://www.mdpi.com/2073-4344/10/2/172/s1>, Figure S1. DSC curves of Fe-BTC before (fresh) and after reaction (used), Figure S2. Adsorption isotherm of N₂, inset: micropore size distribution by BHJ method of Fe-BTC after reaction (used).

Author Contributions: Conceptualization, A.D.S.-A., S.M.V.-D., M.B. and A.Q.; Data curation, A.D.S.-A., G.V., D.M.-R. and A.Q.; Formal analysis, A.D.S.-A., G.V., D.M.-R. and A.Q.; Funding acquisition, J.A.C. and S.M.V.-D.; Investigation, A.D.S.-A., G.V., S.M.V.-D., F.T., M.B. and A.Q.; Methodology, A.D.S.-A., G.V., S.M.V.-D., F.T. and A.Q.; Project administration, J.A.C., S.M.V.-D. and A.Q.; Supervision, J.A.C., S.M.V.-D., M.B. and A.Q.; Validation, A.D.S.-A., G.V. and S.M.V.-D.; Visualization, S.M.V.-D. and A.Q.; Writing – original draft, A.D.S.-A. and A.Q.; Writing – review & editing, A.D.S.-A., G.V., J.A.C., S.M.V.-D., F.T., M.B. and A.Q. All authors have read and agreed to the published version of the manuscript.

Funding: The authors thank the financial support by Consejo Nacional de Ciencia y Tecnología (CONACYT) for the grant number 764635 and the project 256296; and to TNM for the supporting project 5627.19.P. Also, to the Spanish Ministerio de Ciencia, Innovación y Universidades (MICINN) and FEDER program (EU) through the projects: CTM2016-76454-R (MICINN) and RTI2018-095052-B-I00 (MCIU/AEI/FEDER, UE).

Acknowledgments: The authors thank Alvaro Perez for his technical assistance, and Dr. Pascual Bartolo Pérez and Eng. Willian Cauch Ruiz for the characterization and interpretation of the XPS spectrum.

Conflicts of Interest: The authors declare no conflict of interest.

References

- Romano, U.; Ricci, M. Industrial Applications. In *Liquid Phase Oxidation via Heterogeneous Catalysis: Organic Synthesis and Industrial Applications*; Clerici, M.G., Kholdeeva, O.A., Eds.; John Wiley & Sons, Inc.: Hoboken, NJ, USA, 2013; pp. 451–506. ISBN 9780470915523.
- Karakhanov, E.A.; Maximov, A.L.; Kardasheva, Y.S.; Skorkin, V.A.; Kardashev, S.V.; Ivanova, E.A.; Lurie-Luke, E.; Seeley, J.A.; Cron, S.L. Hydroxylation of Phenol by Hydrogen Peroxide Catalyzed by Copper(II) and Iron(III) Complexes: The Structure of the Ligand and the Selectivity of ortho-Hydroxylation. *Ind. Eng. Chem. Res.* **2010**, *49*, 4607–4613. [\[CrossRef\]](#)
- Li, S.; Li, G.; Li, G.; Wu, G.; Hu, C. Microporous carbon molecular sieve as a novel catalyst for the hydroxylation of phenol. *Microporous Mesoporous Mater.* **2011**, *143*, 22–29. [\[CrossRef\]](#)
- Bellussi, G.; Perego, C. Phenol Hydroxylation and Related Oxidations. In *Handbook of Heterogeneous Catalysis*; Major Reference Works; Wiley-VCH Verlag GmbH & Co. KGaA: Weinheim, Germany, 2008; pp. 3538–3547. ISBN 9783527610044.
- Perego, C.; Millini, R. Porous materials in catalysis: challenges for mesoporous materials. *Chem. Soc. Rev.* **2013**, *42*, 3956–3976. [\[CrossRef\]](#) [\[PubMed\]](#)
- Liu, H.; Lu, G.; Guo, Y.; Guo, Y.; Wang, J. Deactivation and regeneration of TS-1/diatomite catalyst for hydroxylation of phenol in fixed-bed reactor. *Chem. Eng. J.* **2005**, *108*, 187–192. [\[CrossRef\]](#)
- Poza-Nogueiras, V.; Rosales, E.; Pazos, M.; Sanroman, M.A. Current advances and trends in electro-Fenton process using heterogeneous catalysts – A review. *Chemosphere* **2018**, *201*, 399–416. [\[CrossRef\]](#) [\[PubMed\]](#)
- Quintanilla, A.; Casas, J.A.; Rodriguez, J. Hydrogen peroxide-promoted-CWAO of phenol with activated carbon. *Appl. Catal. B: Environ.* **2010**, *93*, 339–345. [\[CrossRef\]](#)
- Kavitha, V.; Palanivelu, K. The role of ferrous ion in Fenton and photo-Fenton processes for the degradation of phenol. *Chemosphere* **2004**, *55*, 1235–1243. [\[CrossRef\]](#)
- Choi, J.-S.; Yoon, S.-S.; Jang, S.-H.; Ahn, W.-S. Phenol hydroxylation using Fe-MCM-41 catalysts. *Catal. Today* **2006**, *111*, 280–287. [\[CrossRef\]](#)
- Martínez, F.; Leo, P.; Orcajo, G.; Díaz-García, M.; Sanchez-Sanchez, M.; Calleja, G. Sustainable Fe-BTC catalyst for efficient removal of methylene blue by advanced fenton oxidation. *Catal. Today* **2018**, *313*, 6–11. [\[CrossRef\]](#)
- Li, X.; Wang, B.; Cao, Y.; Zhao, S.; Wang, H.; Feng, X.; Zhou, J.; Ma, X. Water Contaminant Elimination Based on Metal–Organic Frameworks and Perspective on Their Industrial Applications. *ACS Sustain. Chem. Eng.* **2019**, *7*, 4548–4563. [\[CrossRef\]](#)
- Bhattacharjee, S. Hydroxylation of benzene and toluene by heterogeneous iron metal-organic framework (Fe-BTC). *Indian J. Chem. -Section A* **2018**, *57*, 778–783.
- Zhen, W.; Li, B.; Lu, G.; Ma, J. Enhancing catalytic activity and stability for CO₂ methanation on Ni@MOF-5 via control of active species dispersion. *Chem. Commun.* **2015**, *51*, 1728–1731. [\[CrossRef\]](#) [\[PubMed\]](#)
- Lv, H.; Zhao, H.; Cao, T.; Qian, L.; Wang, Y.; Zhao, G. Efficient degradation of high concentration azo-dye wastewater by heterogeneous Fenton process with iron-based metal-organic framework. *J. Mol. Catal. A: Chem.* **2015**, *400*, 81–89. [\[CrossRef\]](#)

16. Gao, Y.; Li, S.; Li, Y.; Yao, L.; Zhang, H. Accelerated photocatalytic degradation of organic pollutant over metal-organic framework MIL-53(Fe) under visible LED light mediated by persulfate. *Appl. Catal. B: Environ.* **2017**, *202*, 165–174. [[CrossRef](#)]
17. Tsai, F.-C.; Xia, Y.; Ma, N.; Shi, J.-J.; Jiang, T.; Chiang, T.-C.; Zhang, Z.-C.; Tsen, W.-C. Adsorptive removal of acid orange 7 from aqueous solution with metal-organic framework material, iron (III) trimesate. *Desalin. Water Treat.* **2016**, *57*, 3218–3226. [[CrossRef](#)]
18. Sun, Q.; Liu, M.; Li, K.; Zuo, Y.; Han, Y.; Wang, J.; Song, C.; Zhang, G.; Guo, X. Facile synthesis of Fe-containing metal-organic frameworks as highly efficient catalysts for degradation of phenol at neutral pH and ambient temperature. *CrystEngComm* **2015**, *17*, 7160–7168. [[CrossRef](#)]
19. Dhakshinamoorthy, A.; Alvaro, M.; Horcajada, P.; Gibson, E.; Vishnuvarthan, M.; Vimont, A.; Greneche, J.-M.; Serre, C.; Daturi, M.; Garcia, H. Comparison of Porous Iron Trimesates Basolite F300 and MIL-100(Fe) As Heterogeneous Catalysts for Lewis Acid and Oxidation Reactions: Roles of Structural Defects and Stability. *ACS Catal.* **2012**, *2*, 2060–2065. [[CrossRef](#)]
20. Dhakshinamoorthy, A.; Li, Z.; Garcia, H. Catalysis and photocatalysis by metal organic frameworks. *Chem. Soc. Rev.* **2018**, *47*, 8134–8172. [[CrossRef](#)]
21. Kempahanumakkagari, S.; Vellingiri, K.; Deep, A.; Kwon, E.E.; Bolan, N.; Kim, K.-H. Metal-organic framework composites as electrocatalysts for electrochemical sensing applications. *Co-ord. Chem. Rev.* **2018**, *357*, 105–129. [[CrossRef](#)]
22. Zhao, X.; Wang, Y.; Li, D.-S.; Bu, X.; Feng, P. Metal-Organic Frameworks for Separation. *Adv. Mater.* **2018**, *30*, 1705189. [[CrossRef](#)]
23. Li, H.; Wang, K.; Sun, Y.; Lollar, C.T.; Li, J.; Zhou, H.-C. Recent advances in gas storage and separation using metal-organic frameworks. *Mater. Today* **2018**, *21*, 108–121. [[CrossRef](#)]
24. Cheng, M.; Lai, C.; Liu, Y.; Zeng, G.; Huang, D.; Zhang, C.; Qin, L.; Hu, L.; Zhou, C.; Xiong, W. Metal-organic frameworks for highly efficient heterogeneous Fenton-like catalysis. *Co-ord. Chem. Rev.* **2018**, *368*, 80–92. [[CrossRef](#)]
25. Jian, L.; Chen, C.; Lan, F.; Deng, S.; Xiao, W.; Zhang, N. Catalytic activity of unsaturated coordinated Cu-MOF to the hydroxylation of phenol. *Solid State Sci.* **2011**, *13*, 1127–1131. [[CrossRef](#)]
26. Xiang, B.-L.; Fu, L.; Li, Y.; Liu, Y. A New Fe(III)/MOF-5(Ni) Catalyst for Highly Selective Synthesis of Catechol from Phenol and Hydrogen Peroxide. *Chem.* **2019**, *4*, 1502–1509. [[CrossRef](#)]
27. Xiang, B.-L.; Fu, L.; Li, Y.; Liu, Y. Preparation of Fe(II)/MOF-5 Catalyst for Highly Selective Catalytic Hydroxylation of Phenol by Equivalent Loading at Room Temperature. *J. Chem.* **2019**, *2019*, 1–10. [[CrossRef](#)]
28. Bhattacharjee, S.; Choi, J.-S.; Yang, S.-T.; Choi, S.B.; Kim, J.; Ahn, W.-S. Solvothermal synthesis of Fe-MOF-74 and its catalytic properties in phenol hydroxylation. *J. Nanosci. Nanotechnol.* **2010**, *10*, 135–141. [[CrossRef](#)]
29. Sanchez-Sanchez, M.; De Asua, I.; Ruano, D.; Diaz, K. Direct Synthesis, Structural Features, and Enhanced Catalytic Activity of the Basolite F300-like Semiamorphous Fe-BTC Framework. *Cryst. Growth Des.* **2015**, *15*, 4498–4506. [[CrossRef](#)]
30. Thommes, M.; Kaneko, K.; Neimark, A.V.; Olivier, J.P.; Rodríguez-Reinoso, F.; Rouquerol, J.; Sing, K.S. Physisorption of gases, with special reference to the evaluation of surface area and pore size distribution (IUPAC Technical Report). *Pure Appl. Chem.* **2015**, *87*, 1051–1069. [[CrossRef](#)]
31. Dorosti, F.; Alizadehdakhl, A. Chemical Engineering Research and Design Fabrication and investigation of PEBAX / Fe-BTC, a high permeable and CO₂ selective mixed matrix membrane. *Chem. Eng. Res. Des.* **2017**, *136*, 119–128. [[CrossRef](#)]
32. Quintanilla, A.; Casas, J.; Miranzo, P.; Osendi, M.; Belmonte, M. 3D-Printed Fe-doped silicon carbide monolithic catalysts for wet peroxide oxidation processes. *Appl. Catal. B: Environ.* **2018**, *235*, 246–255. [[CrossRef](#)]
33. Centi, G.; Cavani, F.; Trifirò, F. *Selective Oxidation by Heterogeneous Catalysis*; Springer Science & Business Media: New York, NY, USA, 2001; ISBN 1461541751.
34. Liu, H.; Lu, G.; Guo, Y.; Guo, Y.; Wang, J. Chemical kinetics of hydroxylation of phenol catalyzed by TS-1/diatomite in fixed-bed reactor. *Chem. Eng. J.* **2006**, *116*, 179–186. [[CrossRef](#)]

35. Gao, C.; Chen, S.; Quan, X.; Yu, H.; Zhang, Y. Enhanced Fenton-like catalysis by iron-based metal organic frameworks for degradation of organic pollutants. *J. Catal.* **2017**, *356*, 125–132. [[CrossRef](#)]
36. Eisenberg, G. Colorimetric Determination of Hydrogen Peroxide. *Ind. Eng. Chem. Anal. Ed.* **1943**, *15*, 327–328. [[CrossRef](#)]



© 2020 by the authors. Licensee MDPI, Basel, Switzerland. This article is an open access article distributed under the terms and conditions of the Creative Commons Attribution (CC BY) license (<http://creativecommons.org/licenses/by/4.0/>).